İSTANBUL UNIVERSITY CERRAHPAŞA

ORIGINAL ARTICLE
Electrica 2024; 24(2): 357-366

Ultra-narrow Band Fano Resonance-Based All-Dielectric Optical Absorber Using Silica–Silicon Metamaterials

Ali Akbar Mashkour[1,4], Amangaldi Koochaki[1,4], Ali Abdolahzadeh Ziabari[2], Azadeh Sadat Naeimi[3,4]

[1]Department of Electrical Engineering, Aliabad Katoul Branch, Islamic Azad University, Aliabad Katoul, Iran
[2]Nano Research Lab, Lahijan Branch, Islamic Azad University, Lahijan, Iran
[3]Department of Physics, Aliabad Katoul Branch, Islamic Azad University, Aliabad Katoul, Iran
[4]Energy Research Center, Aliabad Katoul Branch, Islamic Azad University, Aliabad Katoul, Iran

Cite this article as: A. Akbar Mashkour, A. Koochaki, A. Abdolahzadeh Ziabari and A. Sadat Naeimi, "Ultra-narrow band fano resonance based all-dielectric optical absorber using silica-silicon metamaterials," *Electrica*, 24(2), 357-366, 2024.

ABSTRACT

In this paper, an optical reflector is designed based on an all-dielectric metamaterial comprising silicon double bars with bent arms positioned on the surface of a silica layer. The proposed structure generates high-quality factor Fano resonance peaks within the visible spectrum, facilitated by the structural asymmetry introduced into the top layer of the metamaterial, i.e., the bar pairs. The use of dielectric materials instead of metal has resulted in lower plasmonic power loss and ultra-high quality factor peaks in the desired range. Simulation results show that the central wavelength, spectral width, and amplitude of the Fano resonance peaks can be adjusted by controlling the geometrical characteristics of the structure. Notably, an ultra-narrow Fano resonance peak of 0.26 nm at 682.78 nm wavelength has been achieved through the geometrical manipulation of the silicon bar pairs. Consequently, the proposed structure holds potential for applications in a variety of optical devices such as ultra-narrow band filters and high-resolution sensors.

Index Terms— All-dielectric meta-material, Fano resonances, high-resolution sensors, optical reflector, ultra-narrow band filters

Corresponding author:
Azadeh Sadat Naeimi

E-mail:
naeimi.a.s@gmail.com

Received: August 21, 2023

Revision Requested: October 19, 2023

Last Revision Received: December 25, 2023

Accepted: January 4, 2024

Publication Date: March 18, 2024

DOI: 10.5152/electrica.2024.23107

I. INTRODUCTION

During the last few years, metamaterial-based plasmonic absorbers have attracted lots of attention and thus, have appeared in many applications such as optical filters [1-3], sensors [4, 5], and optical detectors [6-8]. Many of these applications depend on the resonant nature of metamaterials. In other words, it simply states that the spectral selectivity of the light energy concentration in the near field provided by metamaterial can be used to develop a very high adjustable spectrum shape in terms of absorption factor, as well as crossing- and reflective-wave coefficients. Such high adjustability stems from the powerful electromagnetic field concentrations due to the stimulation of plasmons [9]. The metamaterial-based structures, thanks to their sub-wavelength properties, have gained applications in the construction of very small optical devices [10].

Various efforts have been devoted to improving the performance of metamaterial absorbers, focusing on factors like absorption efficiency, tunability, and quality factor. These aspects are crucial for numerous applications, such as optical communications and sensing. However, many metamaterial absorbers exhibit absorption peaks with low quality factors, attributed not only to Joule loss but also to radiative loss. A straightforward and effective approach to mitigate the radiative loss of metamaterial absorbers involves introducing asymmetry into the structure [9, 11]. This asymmetry leads to the emergence of anti-symmetric resonances known as Fano resonances that are associated with a significant increase in the quality factor of the resonance modes and an extraordinarily large plasmon resonance tunability. This higher quality factor results from the enabled interactions between very narrow dark modes and broad bright modes through symmetry breaking. Besides, the mentioned large tunability is attributed to the high sensitivity of Fano resonances to changes in the characteristics of the surrounding media, such as refractive index and conductivity [9, 11].

Until now, numerous researches have been conducted in the context of Fano resonance-based tunable metamaterial absorbers and reflectors, most of which focused on asymmetric periodic

structures. Zhang et al presented a Fano resonance-based ultra-narrow band perfect absorber in the near-infrared spectrum using double asymmetrically elliptical cylinders [12]. Bauer et al demonstrated that the coupling power of Fano resonances in a metallic photonic crystal can be controlled through variation in the thickness of an intermediary layer—carefully inserted between a golden lattice and an optical waveguide [13]. In [14], a plasmonic wide-band absorber and reflector was proposed using metamaterials in the form of split cruciform mounted next to four rectangular bars to improve absorption as well as achieve highly adjustable Fano peaks. In another research in the same context, a crossed circular configuration with double adjustable resonance peaks was presented and numerically analyzed [15]. Using a combination of L-shape and cruciform structures, in [16], an optical absorber was proposed and its operational features were characterized for different configurations. In a similar study, Li et al showed that all metamaterial-based structures with included asymmetry are capable of providing very sharp Fano peaks [17]. In metamaterials, silver and gold are among the most used metals whose plasmonic power losses are relatively high and, as a result, their spectral selectivity and efficiency are substantially low [18]. To overcome this challenge, all-dielectric metamaterials characterized by significantly low power loss have been suggested. Unlike the plasmonic properties of metals, resonances in all-dielectric metamaterials arise from displacement currents rather than conduction. This fundamental difference results in considerably lower power losses for the desired resonances in all-dielectric metamaterials. [10].

In [18], an all-dielectric metamaterial designed by asymmetrical silicon crossed circles mounted on a silica substrate has been presented; simulation results indicated that due to the closed-circuit current density in the crossed circles, Fano resonance peaks are obtainable within the absorption spectrum of the design. In another research [17], double rectangular cubic silicon bars attached to the top of a substrate of MgF_2 have been used to create Fano resonance peaks in all-dielectric metamaterials; the outcome of the study implied the possibility of achieving ultra-narrow band resonance peaks of nearly 100 percent absorption. Using an asymmetrically elliptical silicon disc on a substrate of silica, Su et al proposed an all-dielectric heuristic structure to realize a refractive index sensor of very high efficiency [19]. In [20], authors suggested a spherical (elliptical) nanoparticle structure with a silicon core and silica cover to attain two Fano resonance peaks in the absorption spectrum. In [21], Liu et al proposed four different topologies using all-dielectric metamaterials in the form of rectangular silicon cubes on a silica layer for sensing applications such as methane gas density detection; their design realized two independent Fano resonance peaks of different sensitivity in the absorption spectrum [21].

There are also other advancements in the field of plasmonic and terahertz metamaterials relying on 3D Dirac semimetals which result in the realization of high-performance optical modulators, lasers, filters, and sensors [22-25]. Another noteworthy development is the introduction of Janus meta-surfaces, a type of metamaterial that has been recently proposed for the creation of high-performance sensors and optical communication systems [26, 27]. Beyond metamaterials, there exist other types of sensors based on multilayer structures, with specific applications in the terahertz region, which present an intriguing area for investigation [28-30].

These studies suggest that the all-dielectric metamaterials not only have a simple construction process, but thanks to their intrinsic property of low emission power loss, they also attain higher power efficiency as compared to the metallic metamaterials. These types of metamaterials have gained great potential in manufacturing optical devices due to advantages such as low price, simple fabrication process, excellent efficiency, and high-quality factor resonance modes.

This paper presents an optical absorber based on the Fano resonance phenomenon using all-dielectric metamaterials in which a pair of silicon double bars with bent arms are mounted on top of a layer of silica insulator that attains resonance peaks of ultra-narrow spectral width. The simulation results demonstrate that introducing asymmetry into the upper layer provides the potential to form asymmetrical Fano resonance peaks with approximately 100% reflection amplitude. These high amplitude peaks are formed due to highly intensified electromagnetic fields within the asymmetrical structures as compared to the symmetrical ones. Furthermore, it will be shown that the amplitude and spectral width of the Fano resonance peaks are perfectly tunable through the manipulation of the geometrical characteristics of the proposed structure. This feature can be viewed as a great potential of the all-dielectric metamaterial-based optical reflectors to be used as a suitable platform for manufacturing such optical devices as ultra-high adjustable modulators, high-resolution sensors, and fast filters. The results of the paper, along with other similar studies, can boost theoretical as well as experimental research toward the full understanding and application of the metamaterial within future technologies.

II. THE PROPOSED STRUCTURE AND OPERATIONAL PRINCIPLE

As shown in Fig. 1, the proposed structure is an arrangement of two all-dielectric layers in which alternating arrays of double silicon bars with bent arms are mounted on a thick substrate of silica. As a light beam is perpendicularly emitted onto the structure, it interacts directly with the surface of the metamaterial, leading to the appearance of asymmetrical Fano resonance peaks within the reflection spectrum of the structure. The central wavelength, amplitude, and bandwidth of the peaks depend upon such parameters as the lengths of the top bars (L_a) and the bent arms (L_b), distance between the two adjacent bars (gap), the thicknesses of the silicon bars (H_a), and the dielectric substrate beneath (H_s). As the structure of the metamaterial consists of an array of similar unit cells, the behavior of the entire structure can be understood by studying the features of a single unit cell.

The initial values of the geometrical parameters of the proposed optical reflector's unit cell have been listed in Table I. These values are chosen so that the absorption spectrum attains a Fano resonance peak within the visible spectrum.

A fabrication method is suggested for the proposed metamaterial as follows: To begin, a silicon film is deposited onto a glass substrate using a technique known as low-pressure physical vapor deposition, forming a thin layer of silicon on the glass. Next, a ZEP520 resist is applied to the sample through a process called spin-coating. The sample is then baked, allowing the resist to settle and create a protective layer. Following this, the meta-surface is crafted using electron beam lithography (EBL), wherein a focused beam of electrons creates a pattern on the resist. Subsequent to EBL, inductively coupled plasma etching is employed to carve out

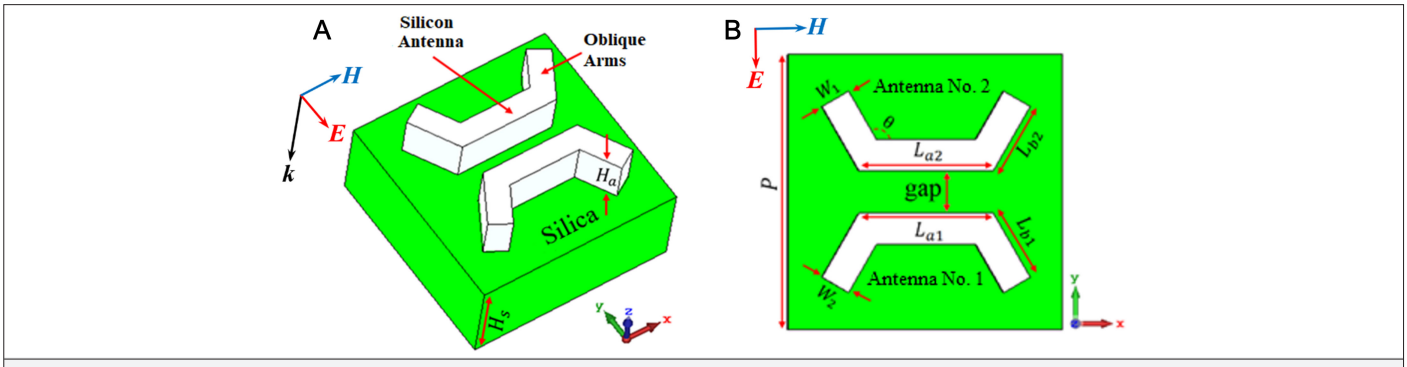

Fig. 1. (a) Three-dimensional and (b) two-dimensional illustration of the upper side of the unit cell of the all-dielectric metamaterial structure. k, E, and H are the incident direction, electric field, and magnetic field vectors, respectively.

the desired structure on the silicon film. This step helps shape the meta-surfaces according to the pattern established by EBL. Finally, upon removing the resist, an oxygen plasma cleaning process is conducted. This crucial step ensures the elimination of any remaining residues or impurities, leaving the fabricated dielectric metamaterial clean and ready for use.

III. THEORY AND SIMULATION METHOD

The proposed structure has been numerically modeled and subsequently simulated using a frequency domain solver in the CST Microwave Studio software package. Throughout the simulation, the boundary conditions are applied to a unit cell in the x and y axes directions while those of the z-axis are left open. The light beam is emitted as a y-polarized transverse electric (TE) plane wave onto the surface of a unit cell. The corresponding absorption spectrum can be computed using the relationship $A = 1 - R - T$, where R and T are, respectively, the reflection and transmission factors conforming to the parameters S_{11} and S_{21}. The relative permittivity of silica is considered 2.25 and that of silicon is equal to 11.68.

TABLE I. THE GEOMETRICAL CHARACTERISTICS OF THE SUGGESTED STRUCTURE IN FIG. 1

Parameter	Symbol	Value
Length of the intermediary arm of the bar 1	L_{a1}	220 nm
Length of the intermediary arm of the bar 2	L_{a2}	220 nm
Length of the oblique arm of the bar 1	L_{b1}	120 nm
Length of the oblique arm of the bar 2	L_{b2}	120 nm
Width of the bar 1	W_1	50 nm
Width of the bar 2	W_2	50 nm
Length and width of the unit cell	P	450 nm
The thickness of the upper layer	H_a	100 nm
The thickness of the silica dielectric layer	H_d	200 nm
Distance between the two adjacent bars	gap	30 nm
The curvature angle of the bar 1 concerning the intermediary arm	θ	45°

IV. ANALYSIS OF THE SIMULATION RESULTS

A. The Fano Resonance Demonstration of The Asymmetrical Structure's Reflection Spectrum

Given Fig. 2 and assuming the geometrical characteristics of the proposed structure with symmetric bars, no absorption peak would appear inside the visible wavelengths (Fig. 3, the black curve).

As expected, changing the angle of one of the silicon bars α_1 (see Fig. 2) leads to an asymmetrical structure; this, in turn, creates a Fano resonance peak at 663 nm wavelength as a result of the interference between the bright and dark modes of the silicon double bar's structure. The structure's absorption is decreased considerably at the wavelength corresponding to the Fano resonance which, subsequently, causes full reflection of the emitted light. Since the interference between the bright and dark modes substantially reduces the emission power loss of the top silicon bars, the resulting Fano resonance peak is characterized by an ultra-high reflection coefficient (around 100%), ultra-narrow bandwidth (less than 0.5 nm), and ultra-high-quality factor.

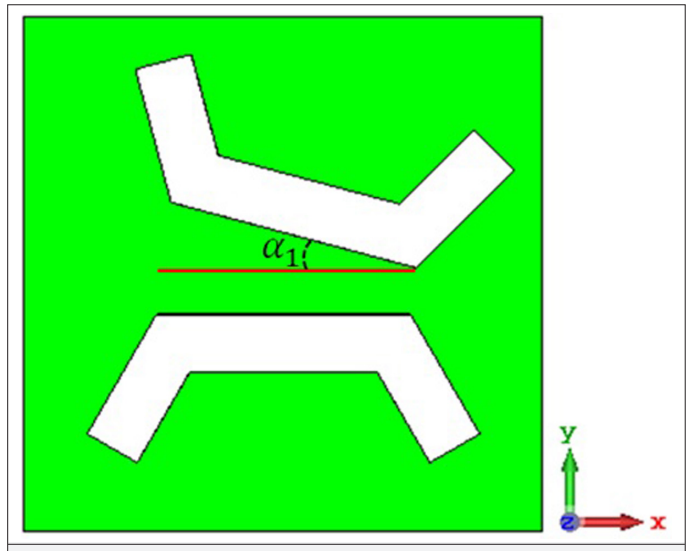

Fig. 2. Asymmetry introduction into the unit cell using angle variation in one of the silicon bar horizontal axis, x, while the other bar remains in its initial position.

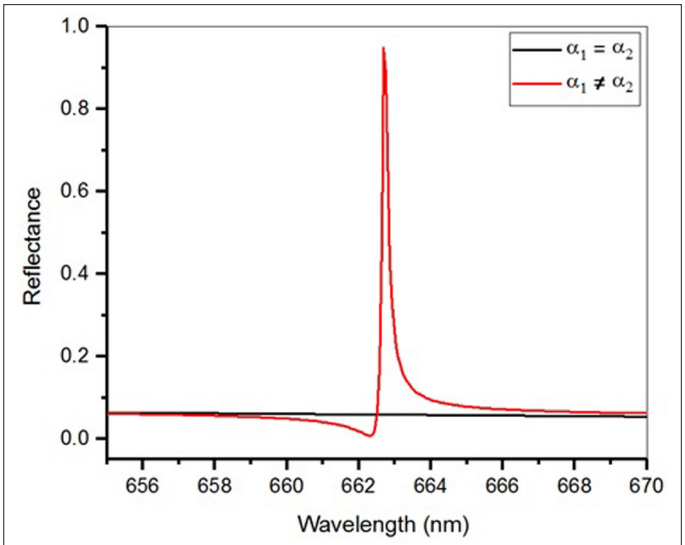

Fig. 3. Reflection spectral comparison of the proposed structure for symmetrical and asymmetrical double silicon bars. The black and red lines correspond to the reflection spectra of the symmetrical and asymmetrical structures.

In order to comprehend the reflection spectral behavior shown in Fig. 3, the z component of the electric field on the boundary of the silica layer and silicon bars is depicted in Fig. 4. From the figure, the charge distributions around bars are symmetrical, illustrating a quadruple resonance pattern. In Fig. 4A and B, the field distributions are shown, respectively, for 662.5 nm and 663.5 nm. As it can be seen from this figure, there are two out-of-phase modes at, consecutively, 662.5 nm and 663.5 nm wavelengths; the interference between these modes results in very low dissipative loss at the corresponding wavelengths; this, in turn, leads to the appearance of a Fano resonance peak of large amplitude and ultra-narrow bandwidth.

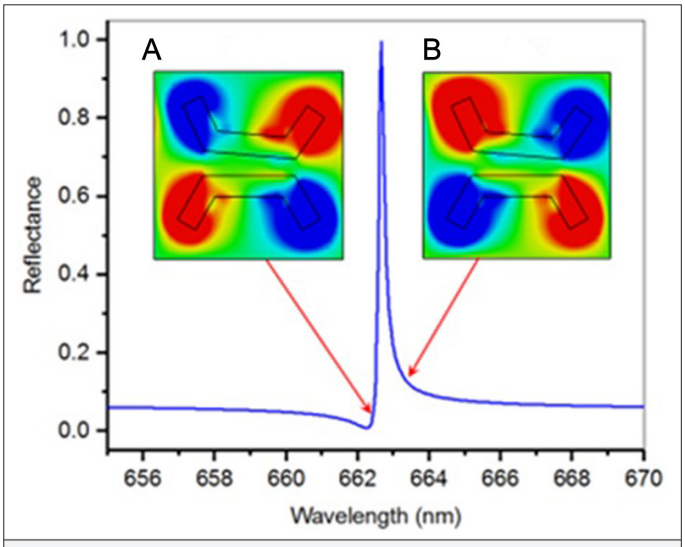

Fig. 4. Appearance of Fano resonance peak around 663 nm wavelength and the z-axis electric field on the boundary of the layer beneath the structure and the silicon bars. Electric field distribution along the z-axis at (a) 662.5 nm and (b) 663.5 nm wavelengths.

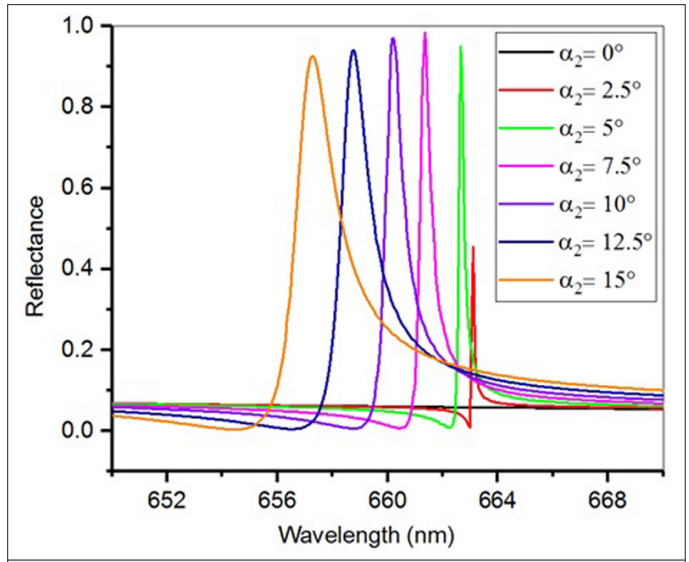

Fig. 5. The structure's reflection spectral variations versus changes in the rotation angle of silicon bars concerning the horizontal axis.

In Fig. 5, the reflection spectral behavior of the proposed structure has been analyzed against variations in the rotation angle of bar2, i.e., α_2, while bar1 remained unchanged. Increasing α_2 shifts the Fano resonance peaks towards smaller wavelengths. Moreover, it can be inferred that any increase in the asymmetry value caused by increasing α_2 from 0 to 7.5 degrees would result in the appearance of a Fano resonance of intensive amplitude; this happens because a scaled-up α_2 creates more structural asymmetry which in turn instills stronger stimulation of the local plasmons of the quadruple dark modes. More elaboration on Fig. 5 reveals that increasing α_2 or equivalently the structural asymmetry gives rise to an elevation of the Full Width of Half Maximum and consequently a reduction of their quality factor. Thus, the quality factor and the degree of structural asymmetry are inversely related [17].

Fig. 5 also shows an initial increase in the Fano resonance peak amplitude, caused by scaled-up α_2, followed by a subsequent reduction. Therefore, based on the preferred absorption amplitude, central resonance wavelength, and spectral width, the rotation angle can be a tuning parameter to adjust appropriately to achieve the desired properties. Table II lists values of the Fano resonance peak central wavelengths corresponding to the related values of α_2.

Among other geometrical parameters of considerable effect on the spectral response, the distance between the two adjacent bars (gap) is another. To quantify the influences of this parameter on resonance peaks, the reflection spectrum of the proposed structure, given $\alpha_2 = 5^{\circ}$, is displayed in Fig. 6 for various gap values.

TABLE II. VALUES OF THE FANO RESONANCE'S CENTRAL WAVELENGTH VERSUS CHANGES IN THE ROTATION ANGLE OF BAR 2 FOR THE HORIZONTAL AXIS X

α_2 (Degree)	2/5	5	7/5	10	12/5	15
λ_f (nm)	663/13	662/65	660/2	661/36	658/75	657/28

α2, the rotation angle of bar 2; Hs, λf, the central wavelength.

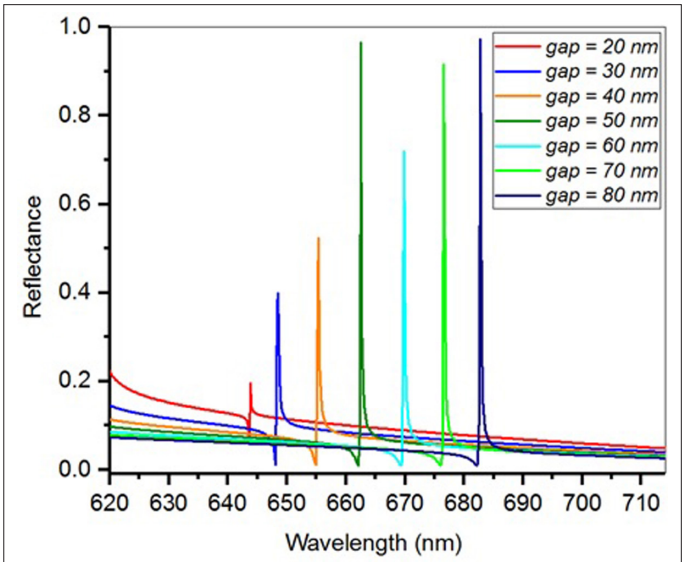

Fig. 6. Effect of distance (gap between the silicon bars) on the reflection spectral variation of the proposed structure. The red curve with the smallest magnitude is related to the minimum value of the gap size, and the dark blue curve possessing the maximum magnitude represents the spectrum of the device with the maximum possible gap size.

From this figure, it can be observed that increasing the gap size, even though it does not affect the peaks' bandwidth noticeably, would shift up the Fano resonance peak's central wavelength. Table III shows the gap values and the corresponding resonance wavelengths. It can be seen that the Fano resonance peaks of the proposed structure have an ultra-narrow reflection spectrum. For example, given a gap of 80nm, a resonance peak of approximately 98% in amplitude at wavelength 682.78nm would appear with an $\Delta\lambda$ equal to 0.26nm. According to the relationship $Q=\frac{\lambda_f}{\Delta\lambda}$, (where λ_f is the central wavelength of the Fano resonance peak and $\Delta\lambda$ is the difference between the wavelength of the peak and depth of the Fano resonance), the quality factor of the resonance peak can reach 2275 which is quite substantial. In [11], the same authors proposed a similar structure to the one suggested here with the difference that the upper layer was one of a metal, the smallest reported $\Delta\lambda$ was 1.87 at 710nm wavelength. The reason behind the considerable downturn of the $\Delta\lambda$ as compared to [11] is that in the upper layer, metal is replaced with dielectrics which leads to a decreased dissipative loss and consequently more sharpened Fano resonance peaks [10].

The height of the silica layer beneath is one of the most important geometrical parameters for directly adjusting the spectral behavior

TABLE III. CENTRAL WAVELENGTHS OF FANO RESONANCE PEAKS VERSUS THE DISTANCE BETWEEN TWO ADJACENT SILICON BARS INSIDE A UNIT CELL

Gap (nm)	20	30	40	50	60	70	80
λ_f (nm)	643/97	648/48	655/37	662/61	669/98	676/75	682/92

Gap, distance between the two bars; λ_f, the central wavelength.

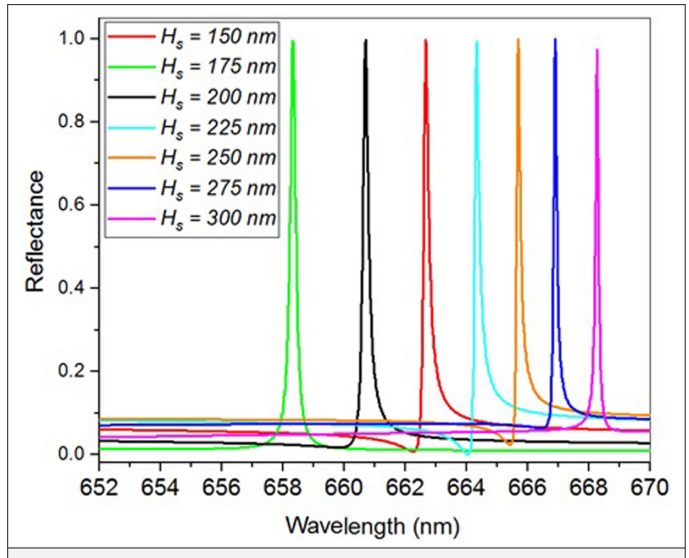

Fig. 7. The reflection spectral variations of the proposed structure versus changes in the thickness of the layer beneath Hs. Hs, the thickness of the dielectric substrate beneath.

of the structure. In Fig. 7, this notion is illustrated over the visible spectrum versus controlled variations in the height of the silica layer.

As the height of the silica layer increases, Fano resonance peaks will be shifted towards larger wavelengths; this, nevertheless, only decreases the peak's amplitude and the spectral bandwidth partially. In Table IV, variation in the Fano resonance peaks' central wavelength is listed versus changes in the thickness of the silica layer. For practical applications of the meta-materials, the reflection behavior of the surface must be stable against variations in the incident angle of the electromagnetic field. The stability of the surface generally depends on the thickness and dielectric material used as the substrate in the structure. The thinner the substrate of the meta-material, the higher the angular stability [31]. Fig. 8 illustrates the angular stability of the proposed metamaterial for TE y-polarized incident plane-wave. According to this figure, as the incident angle increases, the resonance peak shifts toward longer wavelengths, and its magnitude decreases. The proposed structure can function as a good reflector meta-surface for TE-polarized waves up to an incident angle of 10°.

The importance of understanding and harnessing the sensitivity of metamaterials to the polarization angle of incident light lies in the potential to create advanced optical devices, enhance sensing capabilities, and improve the performance of communication systems. The ability to manipulate and control the polarization-dependent responses of metamaterials enables the design of high-performance

TABLE IV. THE CENTRAL WAVELENGTH VARIATION OF THE FANO RESONANCE PEAKS VERSUS CHANGES IN THE THICKNESS OF THE SILICA INSULATOR LAYER

H_s (nm)	150	175	200	225	250	275	300
λ_f (nm)	658/34	660/71	662/67	664/35	665/7	666/92	668/29

Hs, the thicknesses of the dielectric substrate beneath; λf, the central wavelength.

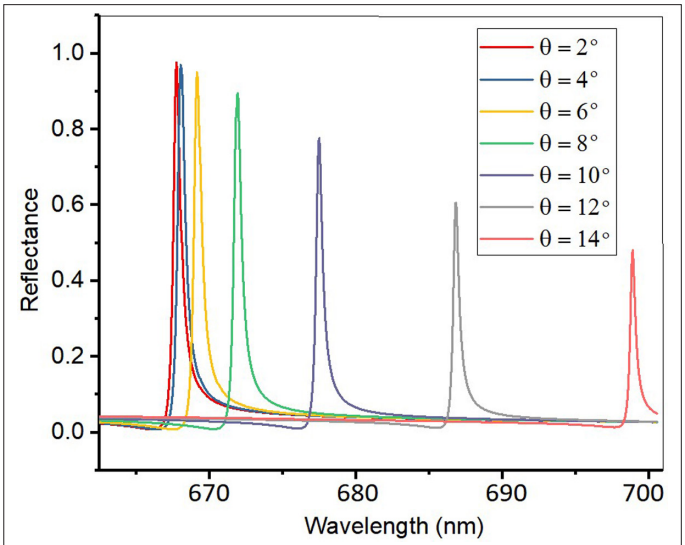

Fig. 8. The influence of incident angle on the reflection spectrum of the proposed meta-material.

devices in the fields of polarimetry, tunable optics, and polarization-sensitive detectors. As shown in Fig. 9, as the polarization angle increases, the magnitude of the Fano resonance peak decreases. Furthermore, it can be concluded that, for polarization angles greater than 60°, the Fano resonance disappears and the spectrum transitions towards a flat profile.

B. The Proposed Structure as a Refractive Index Sensor

The Fano resonance-based metamaterial structures have potential applications in numerous fields, such as the detection of specific substances like gases in the environment. The technical reason behind their application as environmental sensors is the high sensitivity of their Fano resonance to variations in the refractive index within the environment. Hence, they can be used to manufacture sensors of considerable sensitivity and resolution. This section

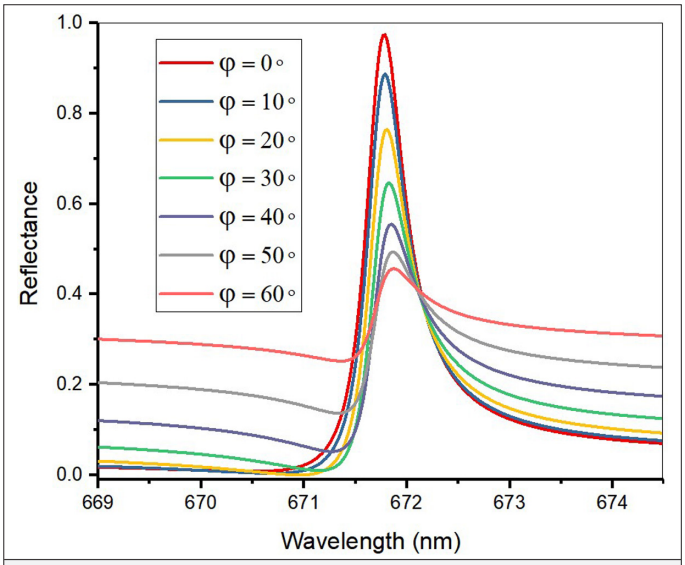

Fig. 9. The influence of changing the polarization angle of the light source on the reflection spectrum of the proposed device.

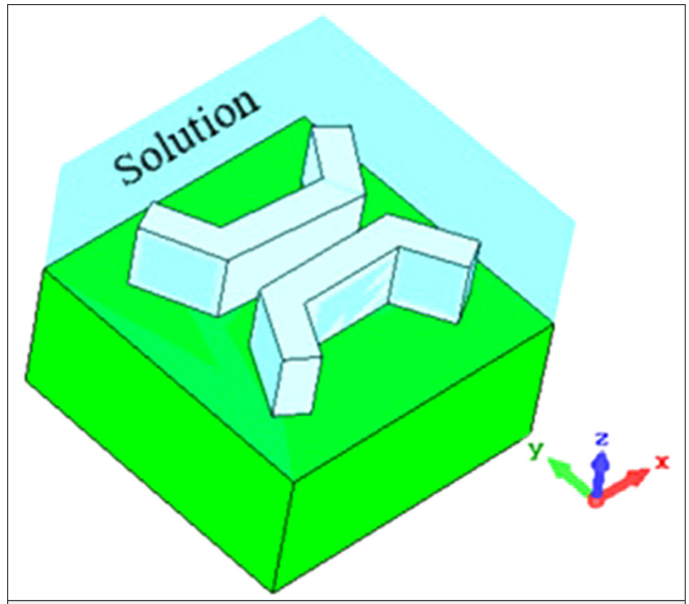

Fig. 10. A three-dimensional illustration of the refractive index sensor created by adding a new solution layer over the proposed structure. It is assumed that the solution covers the top layer of the unit cell.

describes the proposed structure as an environmental sensor. To achieve this, as shown in Fig. 10, an approximately 200 nm dielectric layer with a variable refractive index (as a solution) has been applied to the structure. Then, the corresponding reflection spectral behavior was studied in response to changes in the refractive index of the solution layer.

Fig. 11 shows that increasing the dielectric constant of the solution shifts the Fano resonance peak towards higher wavelengths. Moreover, it can be seen that the spectral width of the related Fano resonance peaks is insensitive to the dielectric constant variations.

Two of the most important effective features of environmental sensors, which are explained in the following, are linearity and sensitivity.

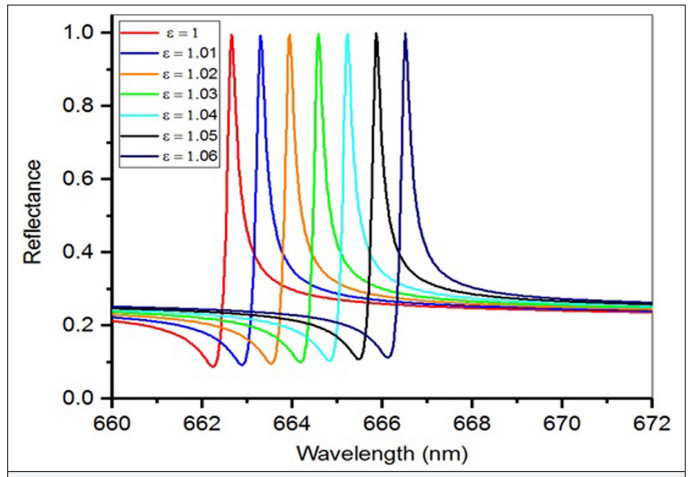

Fig. 11. Reflection spectral variation of the proposed structure versus changes in the environment's dielectric constant.

To characterize these properties for the proposed structure, outputs of the proposed structure must be studied carefully with the appropriate inputs, i.e., environmental refractive index variations. In Fig. 12, spectral locations of the Fano resonance peak, i.e., central wavelength, are displayed as a function of the environment's refractive index. Since sensitivity is proportional to the line's slope in Fig. 10, steeper lines imply higher sensitivity of the structure and thus its better performance as a sensor. The sensitivity of the device, which is defined as the ratio of variations of the resonance wavelength to the refractive index unit (RIU), can be calculated using the following formula [32, 33]:

$$S = \frac{\Delta\lambda_f}{\Delta n} = \frac{\Delta\lambda_f}{\Delta\sqrt{\varepsilon}} \quad (1)$$

where S is the sensor's sensitivity, n, is the refractive index, and Ɛ is the dielectric constant of the environment. Using this relationship, the sensitivity of the proposed structure can be calculated as follows:

$$S = \frac{\Delta\lambda_f}{\Delta\sqrt{\varepsilon}} = \frac{666.5 - 662.63}{\sqrt{1.06} - \sqrt{1}} = \frac{3.87}{0.02956} = 130\frac{nm}{RIU}.$$

If a line's slope changes over different intervals, it should be treated as nonlinearity; thus, as a challenge, it must be compensated for, in case of occurrence, in the subsequent reading system using appropriate software programming. Nonetheless, sensitivity analysis of the proposed structure, as shown in Fig. 12, resulted in a line of constant slope, which suggests perfect linearity of the proposed sensor.

The overall performance of the proposed device could also be evaluated by a parameter called figure of merit (FOM), which represents the optical resolution of the sensor. This parameter is obtained using the following formula [32, 33]:

$$FOM = \frac{S}{\Delta\lambda} \quad (2)$$

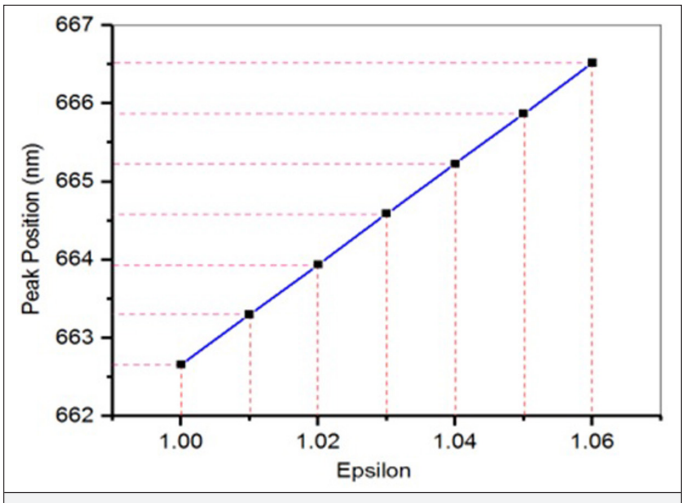

Fig. 12. Central wavelength variation of Fano resonance peak versus changes in the environment's refractive index.

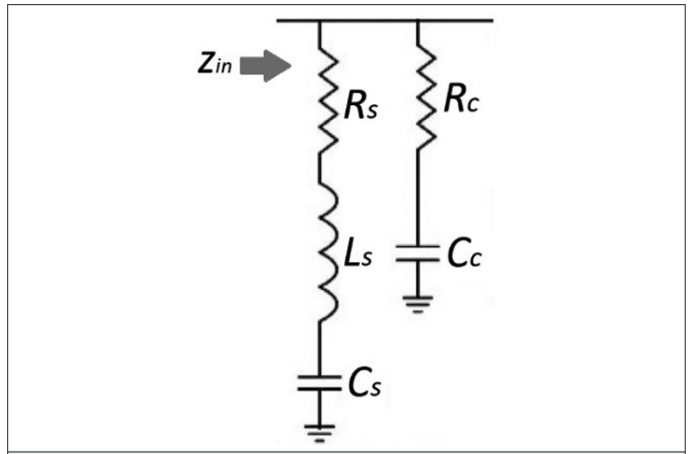

Fig. 13. The simplified equivalent circuit model of the proposed meta-material reflector.

where S is the optical sensitivity expressed by equation 1, and $\Delta\lambda$ is the difference between the peak and dip wavelengths of the Fano resonance. In this context, FOM has been calculated to be approximately 500 RIU^{-1}.

V. EQUIVALENT CIRCUIT MODEL

To better understand the origin of the reflection peak, one can calculate the input impedance of the structure and investigate the impedance matching conditions. This can be achieved by applying transmission line theory and an equivalent circuit model to the studied structure. Given that the Fano resonance line shape is not as simple as dipole resonances, it can only be modeled by a complex high-order equivalent circuit. However, as demonstrated in reference [34], a simplified model consistent with the Fano line shape can be used as the equivalent circuit for every Fano-based metamaterial. The equivalent circuit model of the proposed metamaterial is depicted in Fig. 13.

According to this figure, for $R_S = 0.1\Omega$, $L_S = 35 \times 10^{-6}$ nH, $C_S = 4 \times 10^{-6}$ pF, $R_C = 0.1\Omega$, and $C_S = 7 \times 10^{-6}$ pF at resonance wavelengths of 663 nm, the real part of the input impedance is equal to the free space impedance, and the imaginary part is roughly zero. In other words, reflection peaks appear at wavelengths for which the impedance matching conditions are satisfied. It should be noted that, in the proposed circuit model, the quality factor and magnitude of the resonance peak are directly related to the values of R_S and R_C [34].

VI. COMPARATIVE STUDY

In this section, we present a comparative analysis, assessing the proposed structure in relation to similar studies within the realm of plasmonic and all-dielectric metamaterial sensors [19, 21, 32, 33, 35, 36]. The summary of the comparison is reported in Table V. In this comparison, various optical structures have been employed to realize meta-material reflectors and absorbers. Among the investigated works, our proposed structure exhibits a moderate refractive index sensitivity but has the highest reported FOM. The modest sensitivity is associated with the operational wavelength range of the proposed device, which falls in the visible region. In practical terms, larger operating wavelengths result in greater sensitivity of

TABLE V. COMPARATIVE REVIEW OF THE PROPOSED MICRO-DEVICE AND OTHER SIMILAR STUDIES IN THE FIELD OF PLASMONIC AND ALL-DIELECTRIC METAMATERIALS

Reference	Structure	Sensitivity [nm/RIU]	FOM [RIU^{-1}]
[35]	Nano blocks	306	10.1
[36]	U-shaped cylinder	203	29
[32]	Split-ring	452	56.2
[33]	Rectangular bar with a ring	289	103
[19]	Elliptical cylinders	504	63
[21]	Nano-bar with air hole	1304	277
This paper	Bars with bent arms	130	500

RIU, refractive index unit.

the resonance wavelength to changes in the medium's refractive index. Furthermore, the high value of FOM can be attributed to the narrow line-width of the Fano resonance peak, resulting from the strong enhancement of electromagnetic fields within the gap space between adjacent antennas at the Fano resonance wavelength. Indeed, such a high FOM would turn the proposed device into an extremely accurate sensing system suitable for various applications.

VII. CONCLUSION

In this paper, an all-dielectric metamaterial consisting of a silicon double bar located on top of a silica layer has been presented and numerically investigated. The simulation results suggest that the proposed structure can provide tunable Fano resonance peaks with a high-quality factor within the visible wavelength spectrum. The reason behind the ultra-sharp peaks is the asymmetries introduced into the structure of the silicon double bars, as well as the utilization of dielectrics instead of metals. Furthermore, it has been shown that changes in the geometrical characteristics of the proposed structure, such as the thickness of the dielectric layer, rotation angle of the top silicon bars, as well as refractive index of the surrounding environment, would have considerable effect on the provided central wavelength, spectral width, and amplitude of Fano resonance peaks. Moreover, it has been shown that through adjustment of the geometrical characteristics, a Fano resonance peak with a line-width of approximately 0.26 nm can be achieved at the wavelength of 682.78 nm, which is substantial. Besides, the sensitivity to the environment's refractive index and FOM were calculated to be about 130nm/RIU and 500 RIU^{-1}. Therefore, the suggested structure can be employed in a broad array of applications such as ultra-narrow band filters and detectors and ultra-high-resolution sensors.

Peer-review: Externally peer-reviewed.

Author Contributions: Concept – A.A.Z.; Design – A.K.; Supervision – A.S.N.; Data Collection and/or Processing – A.A.M.; Analysis and/or Interpretation – A.A.M.; Literature Review – A.S.N.; Writing – A.A.M.; Critical Review – A.K.

Declaration of Interests: The authors have no conflict of interest to declare.

Funding: The authors declared that this study has received no financial support.

REFERENCES

1. R. K. Jaiswal, N. Pandit, and N. P. Pathak, "Center frequency and bandwidth reconfigurable spoof surface plasmonic metamaterial band-pass filter," *Plasmonics*, vol. 14, no. 6, pp. 1539–1546, 2019. [CrossRef]
2. Y. Yang *et al.*, "Investigating flexible band-stop metamaterial filter over THz," *Opt. Commun.*, vol. 438, pp. 39–45, 2019. [CrossRef]
3. Y. Fan *et al.*, "Multi-band tunable terahertz bandpass filter based on vanadium dioxide hybrid metamaterial," *Mater. Res. Express*, vol. 6, no. 5, p. 055809, 2019. [CrossRef]
4. Z. Vafapour, "Polarization-independent perfect optical metamaterial absorber as a glucose sensor in food industry applications," *IEEE Trans. Nanobiosci.*, vol. 18, no. 4, pp. 622–627, 2019. [CrossRef]
5. A. Lochbaum *et al.*, "Compact mid-infrared gas sensing enabled by an all-metamaterial design," *Nano Lett.*, vol. 20, no. 6, pp. 4169–4176, 2020. [CrossRef]
6. K. Wang, H. Hu, S. Lu, M. Jin, Y. Wang, and T. He, "Visible and near-infrared dual-band photodetector based on gold–silicon metamaterial," *Appl. Phys. Lett.*, vol. 116, no. 20, 2020. [CrossRef]
7. A. Ahmadivand, B. Gerislioglu, and Z. Ramezani, "Generation of magnetoelectric photocurrents using toroidal resonances: A new class of infrared plasmonic photodetectors," *Nanoscale*, vol. 11, no. 27, pp. 13108–13116, 2019. [CrossRef]
8. M. Oshita, H. Takahashi, Y. Ajiki, and T. Kan, "Reconfigurable surface plasmon resonance photodetector with a MEMS deformable cantilever," *ACS Photonics*, vol. 7, no. 3, pp. 673–679, 2020. [CrossRef]
9. B. Beiranvand, A. S. Sobolev, and A. Sheikhaleh, "A proposal for a dual-band tunable plasmonic absorber using concentric-rings resonators and mono-layer graphene," *Optik*, vol. 223, p. 165587, 2020. [CrossRef]
10. C. Wu *et al.*, "Spectrally selective chiral silicon metasurfaces based on infrared Fano resonances," *Nat. Commun.*, vol. 5, no. 1, p. 3892, 2014. [CrossRef]
11. A. Mashkour, A. Koochaki, A. Abdolahzadeh Ziabari, and A. Sadat Naeimi, "Demonstration of tunable fano resonances in a meta-material absorber composed of asymmetric double bars with bent arms," *Plasmonics*, vol. 17, no. 4, pp. 1607–1618, 2022. [CrossRef]
12. M. Zhang, J. Fang, F. Zhang, J. Chen, and H. Yu, "Ultra-narrow band perfect absorbers based on Fano resonance in MIM metamaterials," *Opt. Commun.*, vol. 405, pp. 216–221, 2017. [CrossRef]
13. C. Bauer, and H. Giessen, "Tailoring the plasmonic Fano resonance in metallic photonic crystals," *Nanophotonics*, vol. 9, no. 2, pp. 523–531, 2020. [CrossRef]
14. M. R. Soheilifar, "Wideband optical absorber based on plasmonic metamaterial cross structure," *Opt. Quantum Electron.*, vol. 50, no. 12, p. 442, 2018. [CrossRef]
15. Z. He *et al.*, "Dual-Fano resonances and sensing properties in the crossed ring-shaped metasurface," *Results Phys.*, vol. 16, p. 103140, 2020. [CrossRef]
16. F. Tavakoli, F. B. Zarrabi, and H. Saghaei, "Modeling and analysis of high-sensitivity refractive index sensors based on plasmonic absorbers with Fano response in the near-infrared spectral region," *Appl. Opt.*, vol. 58, no. 20, pp. 5404–5414, 2019. [CrossRef]
17. X. Long, M. Zhang, Z. Xie, M. Tang, and L. Li, "Sharp Fano resonance induced by all-dielectric asymmetric metasurface," *Opt. Commun.*, vol. 459, p. 124942, 2020. [CrossRef]
18. K. S. Modi, J. Kaur, S. P. Singh, U. Tiwari, and R. K. Sinha, "Extremely high figure of merit in all-dielectric split asymmetric arc metasurface for refractive index sensing," *Opt. Commun.*, vol. 462, p. 125327, 2020. [CrossRef]
19. W. Su, Y. Ding, Y. Luo, and Y. Liu, "A high figure of merit refractive index sensor based on Fano resonance in all-dielectric metasurface," *Results Phys.*, vol. 16, p. 102833, 2020. [CrossRef]
20. R. Reena, Y. Kalra, and A. Kumar, "Ellipsoidal all-dielectric Fano resonant core-shell metamaterials," *Superlattices Microstruct.*, vol. 118, pp. 205–212, 2018. [CrossRef]
21. H. Liu, X. Zhang, B. Zhao, B. Wu, H. Zhang, and S. Tang, "Simultaneous measurements of refractive index and methane concentration through electromagnetic Fano resonance coupling in all-dielectric metasurface," *Sensors (Basel)*, vol. 21, no. 11, p. 3612, 2021. [CrossRef]
22. Y. Cheng, W. Cao, G. Wang, X. He, F. Lin, and F. Liu, "3D Dirac semimetal supported thermal tunable terahertz hybrid plasmonic waveguides," *Opt. Express*, vol. 31, no. 11, pp. 17201–17214, 2023. [CrossRef]
23. G. Wang, W. Cao, and X. He, "3D Dirac semimetal elliptical fiber supported THz tunable hybrid plasmonic waveguides," *IEEE J. Sel. Top.*

Quantum Electron., vol. 29, no. 5: Terahertz Photonics, 1–7, 2023. [CrossRef]
24. X. He, and W. Cao, "Tunable terahertz hybrid metamaterials supported by 3D Dirac semimetals," *Opt. Mater. Express*, vol. 13, no. 2, pp. 413–422, 2023. [CrossRef]
25. X. He, F. Lin, F. Liu, and W. Shi, "3D Dirac semimetals supported tunable terahertz BIC metamaterials," *Nanophotonics*, vol. 11, no. 21, pp. 4705–4714, 2022. [CrossRef]
26. Z. H. Guo, C. J. Gao, and H. Zhang, "Direction-dependent Janus metasurface supported by waveguide structure with spoof surface plasmon polariton modes," *Adv. Mater. Technol.*, vol. 8, no. 2, p. 2200435, 2023. [CrossRef]
27. J. Sui, S. Liao, R. Dong, and H. F. Zhang, "A Janus logic gate with sensing function," *Ann. Phys.*, vol. 535, no. 4, p. 2200661, 2023. [CrossRef]
28. J. Y. Sui, S. Y. Liao, B. Li, and H. F. Zhang, "High sensitivity multitasking non-reciprocity sensor using the photonic spin Hall effect," *Opt. Lett.*, vol. 47, no. 23, pp. 6065–6068, 2022. [CrossRef]
29. S. Guo, C. Hu, and H. Zhang, "Unidirectional ultrabroadband and wide-angle absorption in graphene-embedded photonic crystals with the cascading structure comprising the Octonacci sequence," *J. Opt. Soc. Am. B*, vol. 37, no. 9, pp. 2678–2687, 2020. [CrossRef]
30. S. Y. Liao, Z. Qiao, J. Y. Sui, and H. F. Zhang, "Multifunctional Device for Circular to Linear Polarization Conversion and Absorption." "*Ann. Phys.*, vol. 535, no. 7, p. 2300195, 2023. [CrossRef]
31. B. Khan, S. Ullah, and B. Kamal, "Design and analysis of a wide band cross-polarization converting metasurface,", in Int. Conf. Commun. Technol. (ComTech), IEEE Publications, Vol. 2019, pp. 9–12, 2019.
32. G.-D. Liu *et al.*, "A high-performance refractive index sensor based on Fano resonance in Si split-ring metasurface," *Plasmonics*, vol. 13, no. 1, pp. 15–19, 2018. [CrossRef]
33. Y. Yang, I. I. Kravchenko, D. P. Briggs, and J. Valentine, "All-dielectric metasurface analogue of electromagnetically induced transparency," *Nat. Commun.*, vol. 5, no. 1, p. 5753, 2014. [CrossRef]
34. B. Lv *et al.*, "Analysis and modeling of Fano resonances using equivalent circuit elements," *Sci. Rep.*, vol. 6, no. 1, p. 31884, 2016. [CrossRef]
35. J. Hu, T. Lang, and G. H. Shi, "Simultaneous measurement of refractive index and temperature based on all-dielectric metasurface," *Opt. Express*, vol. 25, no. 13, pp. 15241–15251, 2017. [CrossRef]
36. M. Qin *et al.*, "Electromagnetically induced transparency in all-dielectric U-shaped silicon metamaterials," *Appl. Sci.*, vol. 8, no. 10, p. 1799, 2018. [CrossRef]

AliAkbar Mashkour Ph.D. candidate in electronic engineering, from Islamic Azad University Aliabad Katoul Branch, Science 2016.

Amangaldi Koochaki He received the B.S in electrical engineering from Tehran University, Iran. He received M.S and Ph.D. from Amirkabir University of Technology, Tehran, Iran. Currently, he is an assistant professor in Aliabad Katoul Branch of Islamic Azad University. His research interests are power system analysis and protection, FACTS, smart grids, and artificial intelligence in power system.

Ali Abdolahzadeh Ziabari, Ph.D in solid state physics. Faculty member of Islamic Azad University of Lahijan. His research field is optoelectronic devices, nanostructured devices, and first principle studies.

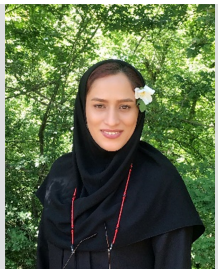

Azadeh Sadat Naeimi Dr Azadeh Sadat Naeimi received her Ph.D. degree in Condensed Matter Physics, 2013 from Islamic Azad University, Science and Research branch, TEHRAN, Iran. she is working as Associate Professor in Department of Electrical Engineering of Islamic Azad University Aliabad Katoul Branch, Iran, since 2008. Her research interests include Magnetic Properties of Multiferroic Nanopowders, Transport properties and Optical Absorber.